# Axonal Growth during Regeneration: A Quantitative Autoradiographic Study

ALAN TESSLER, LUCILA AUTILIO-GAMBETTI, and PIERLUIGI GAMBETTI
*Department of Neurology, The Medical College of Pennsylvania, Philadelphia, Pennsylvania 19129, and Division of Neuropathology, Institute of Pathology, Case Western Reserve University, Cleveland, Ohio 44106*

ABSTRACT The intraaxonal distribution of labeled glycoproteins in the regenerating hypoglossal nerve of the rabbit was studied by use of quantitative electron microscope autoradiography. 9 d after nerve crush, glycoproteins were labeled by the administration of [$^3$H]fucose to the medulla. The distribution of transported $^3$H-labeled glycoproteins was determined 18 h later in segments of the regenerating nerve and in the contralateral, intact nerve. At the regenerating tip, the distribution was determined both in growth cones and in non-growth cone axons, 6 and 18 h after labeling. The distribution within the non-growth cone axons of the tips was quite different at 6 and 18 h. At 6 h, the axolemma region contained <10% of the radioactivity; at 18 h, it contained virtually all the radioactivity. In contrast, the distribution within the growth cones was similar at both time intervals, with 30% of the radioactivity over the axolemmal region. Additional segments of the regenerating nerve also showed a preferential labeling of the axolemmal region. In the intact nerve, $^3$H-labeled glycoproteins were uniformly distributed. These results suggest that: (*a*) in this system the labeled glycoproteins reaching the tip of the regenerating axons are inserted into the axolemma between 6 and 18 h after leaving the neuronal perikaryon; (*b*) at the times studied, there is a fairly constant ratio between glycoproteins reaching the growth cone through axoplasmic transport and glycoproteins inserted into the growth cone axolemma; (*c*) the axolemma elongates by continuous insertion of membrane precursors at the growth cone; the growth cone then advances, leaving behind an immature axon with a newly formed axolemma; and (*d*) glycoproteins are preferentially inserted into the axolemma along the entire regenerating axon.

It is well known that components necessary for the elongation of the plasma membrane in regenerating axons are synthesized in the neuronal cell body and delivered through fast axoplasmic transport (reviewed in reference 21). However, little information is available concerning the site of insertion of the precursors into the axolemma and the mechanism of axonal elongation. According to one hypothesis, supported by in vitro studies, new membrane addition occurs only at the growth cone (5), yet electron microscope autoradiographic (EMA) studies of regenerating nerve have shown that proteins transported to the growth cone are located predominantly beneath the axolemma rather than preferentially within it (22, 25). Another hypothesis holds that rapidly transported materials are inserted into the axolemma not only at the growth cone, where axolemmal elongation occurs, but also at other sites along the growing axon, as part of the process of axolemmal enlargement or maturation (4, 8).

Glycoproteins are components of neuronal membrane systems, including the axolemma, which are supplied to the axon by fast axoplasmic transport after synthesis and assembly in the cell body (reviewed in reference 20). During the period of active axonal outgrowth after axotomy, increased amounts of glycoproteins are transported along the regenerating hypoglossal nerve (13–16). The increased delivery of glycoproteins during regeneration presumably reflects an augmented demand for membrane precursors at the site of incorporation into newly forming axolemma. Glycoproteins are therefore excellent markers to study the formation of new axolemma during axonal regeneration.

We have used quantitative EMA to investigate the intraaxonal distribution of transported glycoproteins in various segments of a regenerating nerve, including the tip and segments proximal and distal to the site of crush. At the regenerating tip we have analyzed the glycoprotein distribution both in the

THE JOURNAL OF CELL BIOLOGY · VOLUME 87 OCTOBER 1980 197-203

growth cones and in the non-growth cone axons, which represent the axonal segment immediately proximal to the growth cone. In our study of these two portions of the axon in the regenerating tip, we recognize the implication of in vitro studies (5) that membrane addition is a complex process that cannot be adequately understood by studying one axonal segment only. Two time intervals, 6 h and 18 h, were chosen to investigate the location of glycoproteins shortly after their arrival and after they have had time to be distributed.

Finally, we have also examined the distributions of transported glycoproteins in precrush and postcrush segments and compared them to that of the contralateral intact nerve, because observations of regenerating nerve (4) and of growing cultured axons (8) have suggested that rapidly transported proteins are inserted into the axolemma along the axon as well as at the growth cone. The results of this study have been presented in part (35).

## MATERIALS AND METHODS

Five albino rabbits weighing about 2.5 kg were used in these experiments. Surgical procedures were performed under halothane anesthesia. L-[6-$^3$H]fucose (12 Ci/mmol) and L-[5,6-$^3$H]fucose (58.6 Ci/mmol) were obtained from New England Nuclear, Boston, Mass.

The right hypoglossal nerve was crushed twice for 30 s, with a 30-s interval, using a jeweler's forceps. The site of crush was at the level of the digastric muscle (~12 mm from the medulla), and was marked by a silk suture sewn into an adjacent muscle.

9 d later, 0.5–1 mCi of L[$^3$H]fucose in 50 μl of saline was injected over a period of 30 min into the midline of the medulla at a depth of 1–2 mm, according to a modification of the method described by Miani (26). The label was applied, using either a single injection into the approximate midpoint of the hypoglossal nuclei or a series of three midline injections along the length of the nuclei. 6 or 18 h later, fixation was carried out either by intracardiac perfusion or by immersion, using 4% paraformaldehyde/1.25% glutaraldehyde in 0.125 M phosphate buffer, pH 7.4, containing 0.2 mM $CaCl_2$. The nerves were removed and dissected into 2-mm segments. All procedures were performed at 4°C. The general distribution of radioactivity along the regenerating and intact nerves and the location of the regenerating tips were determined by liquid scintillation counting (LSC) and light microscope autoradiography. Nerve segments were bisected longitudinally: one half was counted after extraction with 5% TCA; the other half was transferred to fixative, further dissected into 1-mm segments, and processed for plastic embedding. The most distal segments containing a significant amount of radioactivity, as determined by light microscope autoradiography on 1-μm sections, were considered the regenerating tip. TCA-soluble radioactivity, negligible at 18 h after injection, accounted for ~10% of the total radioactivity of the regenerating tip at 6 h. To ensure that all unincorporated fucose had been released from the 6 h nerve segments during fixation, fixatives were changed until no radioactivity was detected by LSC. Segments of nerve were postfixed in 1% buffered $OsO_4$, dehydrated in graded ethanols, and embedded in Araldite 502.

Light and electron microscope autoradiograms were prepared according to the technique of Salpeter et al. (30, 31), as described previously (19). Sections from the experimental (operated) and intact (unoperated) nerves were mounted on the same slide. EM autoradiograms were developed in Elon ascorbic acid with latensification (32). All axon-myelin-Schwann cell complexes present in a given area and containing two or more silver grains were photographed (regardless of the location of the grains), and the negatives were enlarged to a final magnification of × 28,000. EM autoradiograms were analyzed for the following time intervals and nerve segments: (*a*) 6 h regenerating tip (two animals); (*b*) 18 h regenerating tip (three animals); (*c*) 18 h postcrush segment located ~11 mm proximal to the tip and ~4 mm distal to the crush (one animal); (*d*) 18 h precrush segment located 4–6 mm proximal to the crush (three animals); and (*e*) 18 h intact nerve equidistant with the regenerating tip (one animal). For the 6 and 18 h tips, the axon population was divided into two groups that were analyzed separately. One group included the growth cones, defined as axons containing five or more cisterns or vesicles and/or finely granular material. The second group included axons immediately proximal to the growth cones; these axons were generally thin, contained neither cisterns nor vesicles, and are referred to as non-growth cone axons. In the postcrush segment only non-growth cone axons with a radius of 640 nm or more (≥4 HD)[1] were analyzed to select a homogeneous population of relatively mature axons. Axons 640 nm or more in radius were also used in other segments except that the non-growth cone axons had a radius of 320 nm or more (≥2 HD).

The distribution of the radioactivity within the axon was analyzed following a method we have previously described in detail (17, 18). Briefly, the exact distance from the axolemma of each silver grain, located inside or immediately outside the axon, was established (6). Grains were then tabulated according to their location in various concentric compartments 160 nm (1 HD) wide, around the axolemma. A similar procedure was followed for random points (17).

Grain densities for each of these compartments were obtained by dividing the number of grains by the corresponding number of random points, and histograms of experimental grain density distributions were constructed. Scattered radiation from adjacent axons was corrected by excluding from the analysis grains and points shared by two or more axons up to a distance of 640 nm (4 HD) from the axolemma (18). Because no statistically significant differences were found when histograms derived from corresponding nerve segments of different animals were compared, data from all animals were combined to obtain only one histogram for each segment and time studied. These experimental histograms were compared with the series of theoretical curves for radioactive sources of comparable radius provided by Salpeter et al. (32), to analyze further the distribution of the radioactivity. The average axonal radius of each experimental group was determined by use of the formula: radius = 3.42 $x$, where $x$ is the distance from the axolemma into the axon within which half the total random points fall (6). For some histograms the theoretical curves for rounded radioactive sources containing radioactivity uniformly distributed (solid disks) and the theoretical curves for sources with the radioactivity selectively concentrated at the periphery (hollow circles) were combined in different ratios to find the best fit for the experimental data (32). The relative contributions ($r$) to the experimental densities made by a uniformly distributed radioactive component and by one that is selectively concentrated at the periphery were calculated from these best fitting composite theoretical curves using the formula: $r = q/DR\ (1-q)$ (6, 32), where $DR$ is a density ratio that depends on the size of the source (Fig. 17 of reference 32) and $q$ and $1-q$ are fractional representations of the theoretical curves corresponding to the solid disk ($q$) and to the hollow circle ($1-q$).

Standard errors in the histograms were calculated by use of the formula: $G/P\ \sqrt{1/G + 1/P}$, where $G$ = number of silver grains and $P$ = number of random points for each compartment (6).

## RESULTS

The typical distribution of the transported labeled glycoproteins, as determined by LSC, along the intact and regenerating hypoglossal nerves 18 h after local administration of [$^3$H]fucose to the XII nerve nuclei is illustrated in Fig. 1. In the intact nerve the radioactivity is evenly distributed along the entire length of the nerve examined. The contralateral regenerating nerve contains up to four times more radioactivity distributed

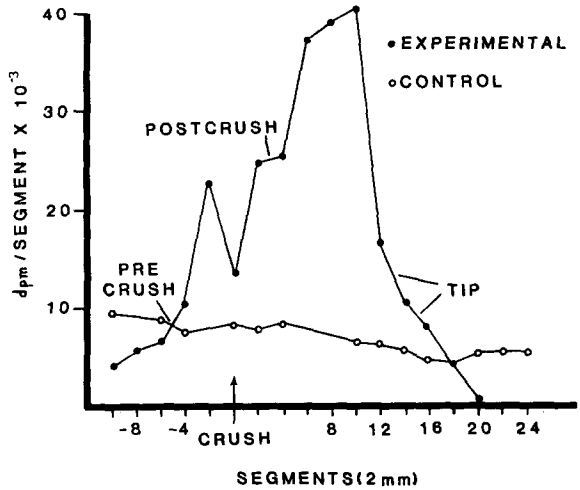


FIGURE 1 Typical distributions of radioactivity along intact and regenerating hypoglossal nerves 18 h after administration of [$^3$H]-fucose to the XII nerve nuclei, as determined by liquid scintillation counting. Solid circles, right hypoglossal nerve crushed 9 d before labeling. Open circles, intact nerve from the same rabbit. The segments used for autoradiography are indicated.

[1] 1 HD is an experimental measure of resolution in autoradiography (6, 17, 32). In this study it is equal to 160 nm.

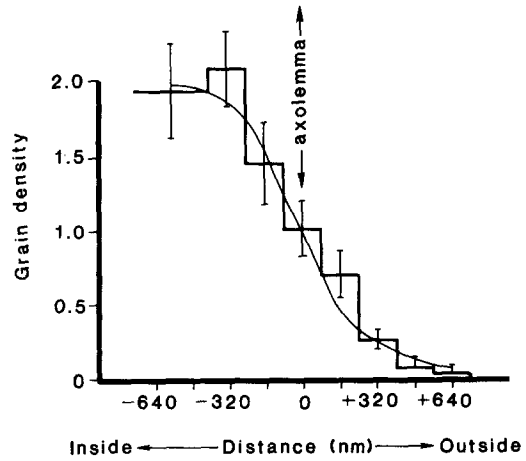


FIGURE 2 Histogram of grain densities over and around axons of intact hypoglossal nerve 18 h after labeling. The superimposed curve fitting the histogram corresponds to the distribution expected if all the radioactivity is uniformly distributed over the cross section of the axon. (Average radius of the axon: 960 nm = 6 HD; based on 160 grains).

in two unequal peaks. The first peak is located 2 mm proximal to the point of crush; the second, much larger peak is 6–10 mm distal to the point of crush. It is followed by a sudden drop of the radioactivity, which is reduced to background level ~8 mm from the major peak.

## EMA

GENERAL OBSERVATIONS: The distribution of the silver grains in all segments of intact and regenerating nerves examined both at 6 and 18 h after administration of [$^3$H]fucose indicated that labeled glycoproteins are present only in the axons and not in the myelin or in the Schwann cells.

The histogram of the silver grain densities over and around the axons of the 18 h intact nerve is shown in Fig. 2. The theoretical curve that best fits this histogram is that of a solid disk. This indicates that the labeled glycoproteins are uniformly distributed within the axons including the axolemmal region.[2] The intraaxonal distribution of radioactivity in the control nerve is significantly different from that of all the segments of the crushed nerves 18 h after [$^3$H]fucose administration (Table I).

The axons of the 18 h precrush segment do not differ morphologically from those of the contralateral unoperated nerve (Fig. 3). However, the axons of this segment show a nonuniform distribution of radioactivity: 23% is located in the axolemmal region and 77% is uniformly distributed over the axons including the axolemma (Fig. 4). The axolemmal region is therefore relatively more labeled than any other axonal compartment.

In the 18-h postcrush segment, which is 4 mm distal to the point of the crush, regenerating unmyelinated sprouts of varying size are present. Among these sprouts are several processes that are identifiable as growth cones. Regenerating sprouts in this segment, as in the most distal segments of the tip, are

[2] Because of the limited resolution of EMA, the term axolemmal region or compartment is used in this study to identify a compartment 160 nm wide, centered on the axolemma. The radioactivity in this compartment is very likely located at the axolemma, although a periaxolemmal location up to ~80 nm from the axolemma cannot be ruled out.

TABLE I

*Statistical Comparison of the Histograms*

| | Distance from axolemma of intraaxonal compartments | | | |
|---|---|---|---|---|
| | 560–720 | 400–560 | 240–400 | 80–240 |
| | nm | | | |
| Intact vs. precrush | NS | $P < .05$ | $P < .01$ | NS |
| Intact vs. postcrush | $P < .01$ | $P < .05$ | $P < .001$ | $P < .02$ |
| Postcrush vs. precrush | $P < .001$ | $P < .05$ | NS | $P < .05$ |
| 6 h Non-growth cones vs. 18 h non-growth cones | — | $P < .05$ | $P < .001$ | $P < .002$ |
| 18 h Non-growth cones vs. 18 h growth cones | — | $P < .002$ | $P < .001$ | $P < .001$ |

Values represent level of significance at various distances from the axolemma. The formula $D_1 - D_2/\sqrt{(SE_1)^2 + (SE_2)^2}$, where $D$ = density and $SE$ = standard error, was used to determine the level of significance. *NS*, not significant.


FIGURE 3 Electron microscope autoradiogram of a myelinated axon from the precrush segment 18 h after infusion of [$^3$H]fucose into the medulla. The axon that contains two silver grains has the appearance of a normal myelinated axon. × 15,600.

generally embedded within Schwann cell cytoplasm, and such regenerating units are surrounded by Schwann cell basal lamina. The axons tabulated, all of which are 640 nm or more in radius (Fig. 5), demonstrate an even more pronounced labeling of the axolemmal region than those of the precrush segment (Fig. 6). About 55% of the radioactivity is related to the axolemmal compartment and the remaining 45% is evenly distributed over the axon. This distribution is significantly different from that of the precrush segment (Table I).

Both the 18 h and 6 h tips contain two morphologically different populations of axonal processes, which were analyzed separately.

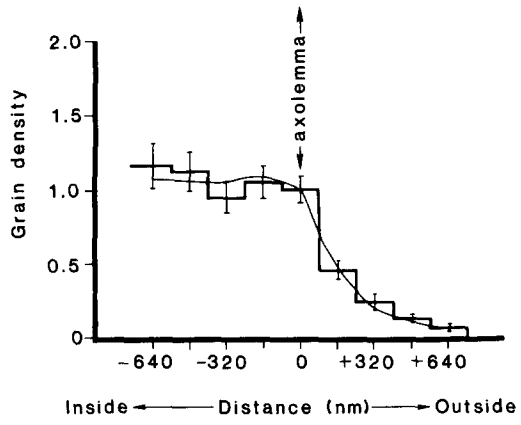


FIGURE 4 Histogram of grain densities over and around axons of precrush segments 18 h after labeling. The superimposed curve fitting the histogram corresponds to the distribution expected if 77% of the radioactivity is uniformly distributed throughout the axons and 23% is concentrated on the axolemma. (Average radius of the axon: 1,120 nm = 7 HD; based on 564 grains.)

(*a*) Non-growth cone axons consist of fine, unmyelinated processes that contain mitochondria, clear vesicular material, and neurotubules, but few neurofilaments. In the 18 h non-growth cone axons, radioactivity is found only over the axolemmal region (Fig. 7). This distribution contrasts markedly with that seen at 6 h, when ~93% of the radioactivity is uniformly distributed over the axon (Fig. 7).

(*b*) Growth cones contain five or more cisterns or vesicles and/or finely granular material, but frequently include vesicular and smooth membranous structures in large quantities (Fig. 8). Filopodia were not observed.

The distribution of radioactivity in the growth cones is very similar both at 6 and 18 h after administration of labeled fucose (Fig. 9). The theoretical curve that fits the experimental data is that obtained by a combination of a solid disk and an annulus. The data are compatible with the distribution expected if 70% of the radioactivity is uniformly distributed over the growth cones and 30% is concentrated on a 160-nm (1 HD) annulus with its outer edge at the axolemma. This distribution is significantly different from that of the 18 h non-growth cone axons (Table I).

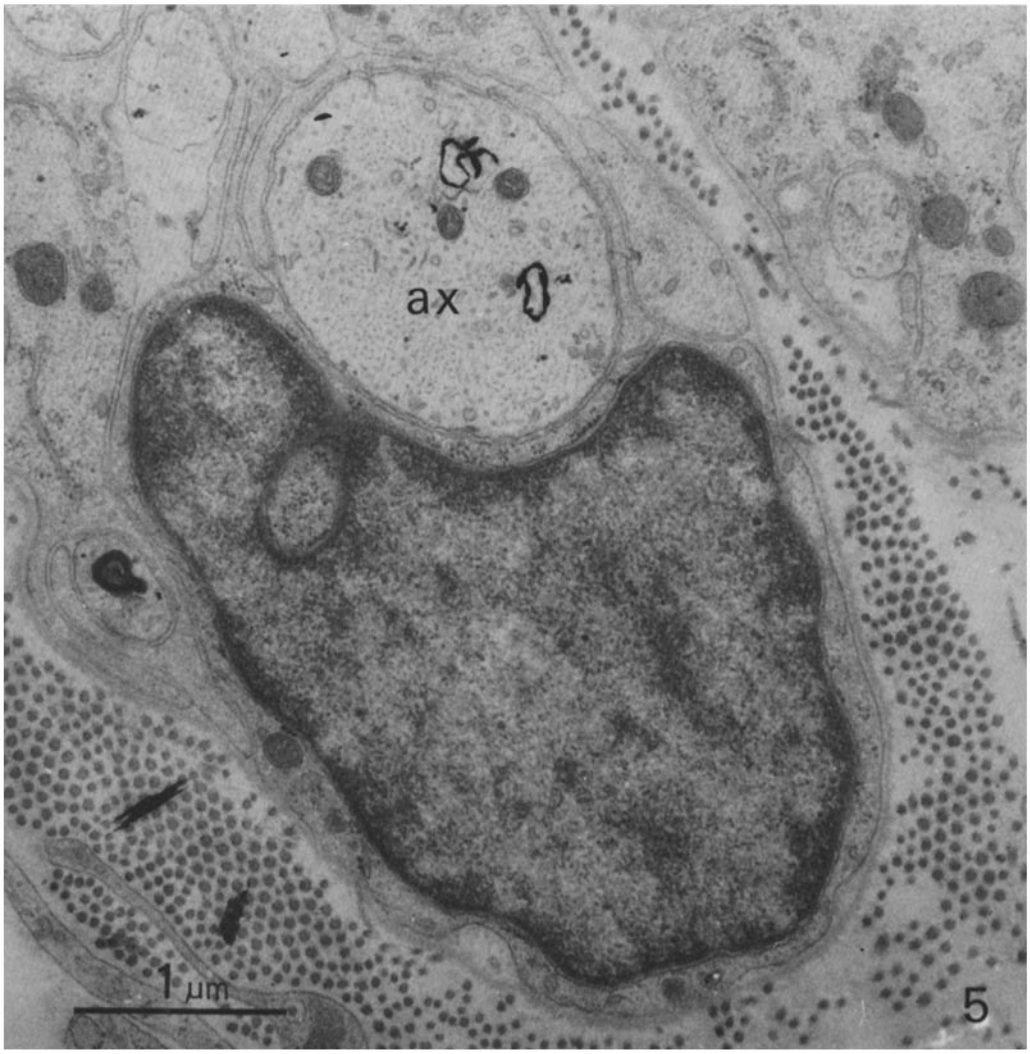


FIGURE 5 Electron microscope autoradiogram of a regenerating unit from the postcrush segment 18 h postinjection. Note the fairly mature appearance of the axon (*ax*) and the overlapping Schwann cell processes indicating the beginning of myelination. Only axons of this type, ≥640 nm in radius, were used in building the histogram. × 28,400.

## DISCUSSION

The main finding of the present study is the striking difference in the distribution of $^3$H-labeled glycoproteins in non-growth cone axons of the regenerating tip 6 and 18 h after injection of [$^3$H]fucose: at 6 h the $^3$H-labeled glycoproteins are uniformly distributed over these axons; at 18 h they are found only over the region of the axolemma. These results indicate that $^3$H-labeled glycoproteins reaching the tip of the regenerating axons by axoplasmic transport are inserted into the axolemma between 6 and 18 h.

While the distribution of $^3$H-labeled glycoproteins in the non-growth cone axons is very different at 6 and 18 h, the distribution in the growth cones does not show any significant change during this time period: 70% of the radioactivity remains uniformly distributed and 30% located in the axolemmal region.

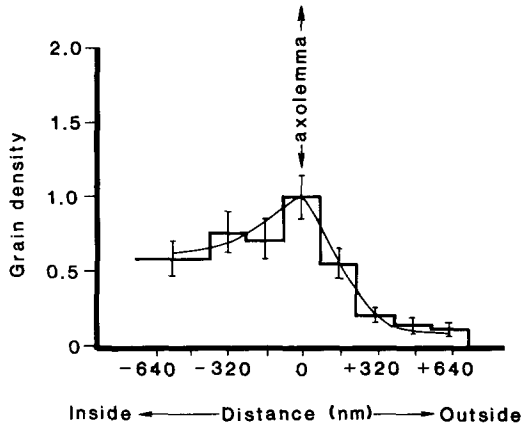


FIGURE 6 Histogram of grain densities over and around axons of the postcrush segment 18 h after labeling. The superimposed curve that fits the histogram corresponds to the distribution expected if 45% of the radioactivity is uniformly distributed and 55% is concentrated on the axolemma. (Average radius of the axon: 937.6 nm = 5.86 HD; based on 240 grains.)

One possible explanation of these findings is the following. When they reach the growth cone, glycoproteins are inserted into the growth cone axolemma at such a rate that, after the build up of a sizable pool, a fairly constant ratio is maintained between glycoproteins provided to the growth cone by axoplasmic transport and glycoproteins removed from the axoplasm both by insertion into the axolemma and by retrograde transport (1, 13). By the continuous insertion of glycoproteins (as well as other molecules) into the axolemma, the growth

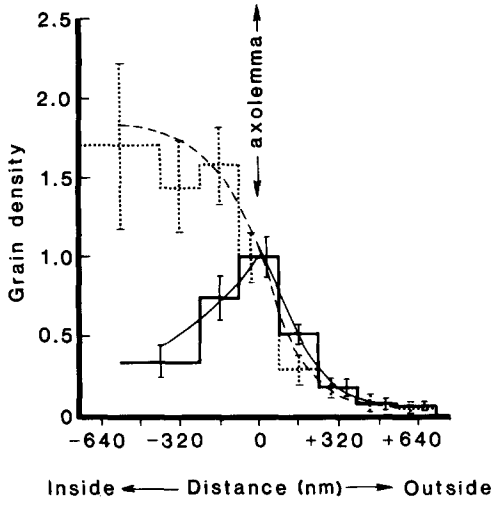


FIGURE 7 Histograms of distribution of grain densities over and around non-growth cone axons of the regenerating tip 6 h (---) and 18 h (—) after labeling. The theoretical curve (---) fitting the experimental histogram of the 6 h non-growth cone axons corresponds to the curve expected if 93% of the radioactivity is uniformly distributed throughout the axon. The theoretical curve (—) fitting the experimental histogram of the 18-h non-growth cone axons corresponds to the curve expected if 100% of the radioactivity is concentrated on the axolemma. (Average radius of the axon: 6 h, 552 nm = 3.45 HD; 18 h, 496 nm = 3.1 HD; 6 h based on 210 grains; 18 h based on 228 grains.)

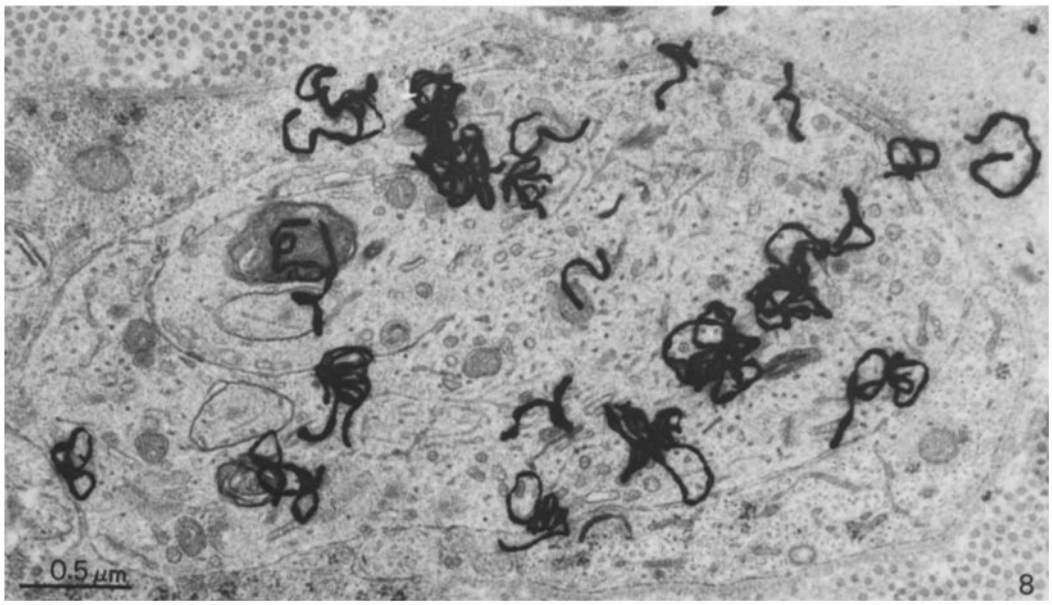


FIGURE 8 Electron microscope autoradiogram of a typical growth cone from the regenerating tip 6 h postinjection. The heavily labeled process contains vesicular and smooth membranous profiles in great profusion. × 31,400.

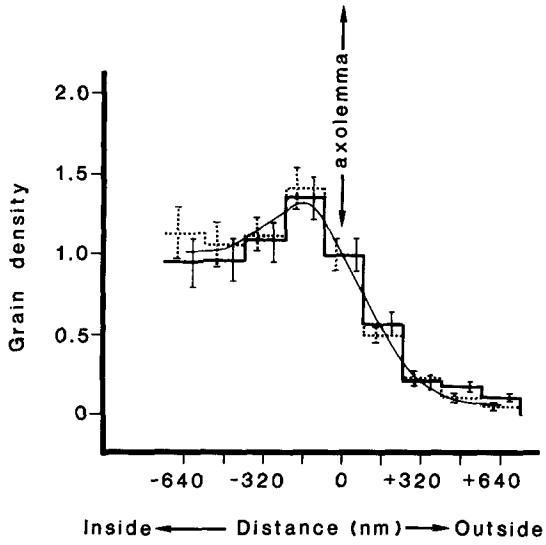


FIGURE 9 Histograms of distribution of grain densities over and around growth cones of the regenerating tip 6 h (---) and 18 h (—) after labeling. The theoretical curve (—) fitting both experimental histograms corresponds to that expected if 70% of the radioactivity is uniformly distributed over the growth cones and 30% is concentrated on a 160-nm (1-HD) annulus with its outer edge at the axolemma. (Average radius of the axon for both histograms: 1,088 nm = 6.8 HD; 6 h histogram based on 651 grains; 18 h histogram based on 669 grains.)

cone is pushed forward, leaving behind an axon with a newly formed axolemma. The growth cone would therefore be the main site where building material is collected and assembled for the elongation of the axolemma of regenerating axons. A similar mechanism of axon elongation has been proposed for growing sympathetic axons in culture (5). According to this in vitro model, new axolemma would be added to the front of the growth cones in cytoplasmic extensions, the filopodia, and recycled from the more proximal portions of the growth cones. Clearly, it would be of great interest to determine whether elongation of the axolemma occurs by insertion of individual molecules or of preassembled patches of vesicular membranes and whether filopodia are in fact the sites of deposition of new plasma membrane in the regenerating axon. Ours and previous studies provide no answer to these two questions. Filopodia were not seen in our system, nor have they been observed in regenerating goldfish retinal axons (27) or in regenerating sciatic axons (22), but serial sections are needed to exclude their presence (27). In the cell perikaryon, transport of glycoproteins from the Golgi apparatus, where carbohydrate incorporation takes place (3, 34) to the plasma membrane appears to be in the form of intracytoplasmic membranes (2, 10, 11, 20, 36). In elongating axons in vitro, both growth cone axolemma and a population of vesicles found in mounds beneath it are poor in intramembrane particles, suggesting that these vesicles are the source of new axolemma (28, 29). However, this finding has been recently challenged (23).

Previous studies on regenerating axons have demonstrated an accumulation of radioactivity at the tip (12, 13, 15), and EM autoradiography has confirmed that radioactivity is present within the growth cones (22, 25). Our findings are consistent with these studies; but they also indicate that the growth cone is not the only place where glycoproteins are preferentially inserted into the axolemma of the regenerating axon. Although our data on intact nerve and postcrush segments were obtained from only one animal and therefore must be interpreted cautiously, increased amounts of glycoproteins appear to be present on the axolemma of precrush and postcrush segments as compared with the intact nerve. About 23% of the total radioactivity present in the axon is located on the axolemmal region at the precrush segment, whereas in the postcrush segment, the axolemmal radioactivity accounts for 55% of the total. Thus, the distribution of radioactivity in axons of the regenerating nerve shows a proximo-distal increase of labeling of the axolemmal region. This distribution most likely represents an increased rate of glycoprotein insertion into the axolemma of immature axons.

One implication of these findings is that a significant amount of glycoprotein is inserted into the axolemma of relatively mature axons at a considerable distance from the growth cone. Therefore, it appears that in the regenerating nerve, as in elongating nerves in culture (8), glycoproteins are inserted into the axolemma at multiple sites. Freeze-fracture studies of cultured growing axons have shown that the density of intramembrane particles decreases from the perikaryon to the growing tip, suggesting that the newly formed axolemma is immature (28). Hence, it is tempting to postulate that in regenerating axons glycoproteins inserted at the growth cone support the longitudinal growth and those inserted at multiple sites proximal to the tip provide for the lateral growth and maturation of the axolemma. Bisby (4) has offered a similar interpretation of his finding of an increased incorporation of rapidly transported proteins over the entire length of regenerating rat sensory sciatic nerve.

Our observation that the distribution of the axonally transported radioactivity in the precrush segment differs from that of the intact nerve may be attributable to the metabolic changes that take place in the axons proximal to the site of crush during regeneration. The amount of the axonally transported glycoproteins has been reported to be increased 150–240% at 1 wk after axotomy (13, 14, 16), whereas the diameter of the axons of the proximal segment is decreased in regenerating axons (9, 24). These changes may well have an effect on the local metabolism of the axon resulting in a greater insertion of glycoproteins into the axolemma.

Our data show that in the axons of the intact nerve, labeled glycoproteins are uniformly distributed with no preferential location in the axolemma or in the subaxolemmal region. This distribution differs from the nonuniform location of labeled transported protein reported in other quantitative autoradiographic studies, but procedural differences prevent direct comparison of our data with previous findings. Lentz (25) found that the radioactivity was located in a band whose center was 600 nm inside the axolemma of normal portions of regenerating newt nerve. Because this study was carried out 3 d after infusion of leucine, most of the radioactivity very likely represents slowly transported proteins. Byers (7) has reported that in the rabbit unmyelinated vagus nerve, fast transported proteins are confined to a compartment 60–120 nm wide inside the axon; this study, however, was carried out in vitro in desheathed nerves, and the histogram was obtained by combining data from control and colchicine-treated nerves at different times after incubation.

Under the conditions of the present study, 18 h after [$^3$H]-fucose injection, the peak of the migrating $^3$H-labeled glycoproteins has already passed through the nerve segment analyzed, and anterograde transport of the $^3$H-labeled glycoproteins may have largely subsided. Thus, the $^3$H-labeled glyco-

protein distribution that we have observed in axons of both the intact and regenerating nerves at 18 h is probably that of $^3$H-labeled glycoproteins left behind by, rather than transported with, the fast component of axoplasmic flow. This hypothesis is consistent with the previous reports that only a portion of the fast transported material reaches the nerve terminal, while the rest remains in the axon in either a stationary or slowly moving structure (reviewed in reference 33).

We are grateful to Dr. Marion Murray for her critical reading of the manuscript and to Ms. Kathy Weightman for typing the manuscript. Technical help was provided by Mr. R. Artymyshyn and Mr. T. Smayda.

This work was supported by a grant from the Epilepsy Foundation of America to A. Tessler and by U. S. Public Health Service grant NS 14509.

Requests for reprints should be addressed to Dr. P. Gambetti, Division of Neuropathology, Institute of Pathology, Case Western Reserve University, Cleveland, Ohio 44106.

*Received for publication 22 October 1979, and in revised form 9 April 1980.*

## REFERENCES

1. Abe, T., T. Haga, and M. Kurokawa. 1974. Retrograde axoplasmic transport: its continuation as anterograde transport. *FEBS (Fed Eur. Biochem. Soc.) Lett.* 47:272–275.
2. Bennett, G., L. DiGiamberardino, M. L. Koenig, and B. Droz. 1973. Axonal migration of protein and glycoprotein to nerve endings. II. Radioautographic analysis of the renewal of glycoproteins in nerve endings of chicken ciliary ganglion after intracerebral injection of [$^3$H]fucose and [$^3$H]glucosamine. *Brain Res.* 60:129–146.
3. Bennett, G., C. P. Leblond, and A. Haddad. 1974. Migration of glycoprotein from the Golgi apparatus to the surface of various cell types as shown by radioautography after labeled fucose injection into rats. *J. Cell Biol.* 60:258–284.
4. Bisby, M. A. 1978. Fast axonal transport of labeled protein in sensory axons during regeneration. *Exp. Neurol.* 61:281–300.
5. Bray, D. 1973. Model for membrane movements in the neural growth cone. *Nature (Lond.).* 244:93–96.
6. Budd, G. C., and M. M. Salpeter. 1969. The distribution of labeled norepinephrine within sympathetic nerve terminals studied with electron microscope autoradiography. *J. Cell Biol.* 41:21–32.
7. Byers, M. R. 1974. Structural correlates of rapid axonal transport: evidence that microtubules may not be directly involved. *Brain Res.* 75:97–113.
8. Carbonetto, S., and D. M. Fambrough. 1979. Synthesis, insertion into the plasma membrane, and turnover of $\alpha$-bungarotoxin receptors in chick sympathetic neurons. *J. Cell Biol.* 81:555–569.
9. Cragg, B. G., and P. K. Thomas. 1961. Changes in conduction velocity and fibre size proximal to peripheral nerve lesions. *J. Physiol. (Lond.).* 157:315–327.
10. Droz, B., H. L. Koenig, and L. DiGiamberardino. 1973. Axonal migration of protein and glycoprotein to nerve endings. I. Radioautographic analysis of the renewal of protein in nerve endings of chicken ciliary ganglion after intracerebral injection of [$^3$H]lysine. *Brain Res.* 60:93–127.
11. Droz, B., A. Rambourg, and H. L. Koenig. 1975. The smooth endoplasmic reticulum: structure and role in the renewal of axonal membrane and synaptic vesicles by fast transport. *Brain Res.* 93:1–13.
12. Forman, D. S., and R. A. Berenberg. 1978. Regeneration of motor axons in the rat sciatic nerve studied by labeling with axonally transported radioactive proteins. *Brain Res.* 156: 213–225.
13. Frizell, M., W. G. McLean, and J. Sjostrand. 1976. Retrograde axonal transport of rapidly migrating labeled proteins and glycoproteins in regenerating peripheral nerves. *J. Neurochem.* 27:191–196.
14. Frizell, M., and J. Sjostrand. 1974. Transport of proteins, glycoproteins and cholinergic enzymes in regenerating hypoglossal neurons. *J. Neurochem.* 22:845–850.
15. Frizell, M., and J. Sjostrand. 1974. The axonal transport of slowly migrating [$^3$H]leucine labeled proteins and the regeneration rate in regenerating hypoglossal and vagus nerves of the rabbit. *Brain Res.* 81:267–283.
16. Frizell, M., and J. Sjostrand. 1974. The axonal transport of [$^3$H]fucose labeled glycoproteins in normal and regenerating peripheral nerves. *Brain Res.* 78:109–123.
17. Gambetti, P., L. Autilio-Gambetti, N. K. Gonatas, and B. Shafer. 1972. Protein synthesis in synaptosomal fractions. Ultrastructural radioautographic study. *J. Cell Biol.* 52:526–535.
18. Gambetti, P., L. Autilio-Gambetti, B. Shafer, and L. Pfaff. 1973. Quantitative autoradiographic study of labeled RNA in rabbit optic nerve after intraocular injection of [$^3$H] uridine. *J. Cell Biol.* 59:677–684.
19. Gambetti, P., N. A. Ingoglia, L. Autilio-Gambetti, and P. Weiss. 1978. Distribution of [$^3$H]RNA in goldfish optic tectum following intraocular or intracranial injection of [$^3$H] uridine. Evidence of axonal migration of RNA in regenerating optic fibers. *Brain Res.* 154:285–300.
20. Grafstein, B. 1977. Axonal transport: the intracellular traffic of the neuron. *In* Cellular Biology of Neurons, Part I, Handbook of Physiology, Section 1: The Nervous System. Vol. I. E. R. Kandel, editor. Williams & Wilkins Co., Baltimore, MD. 691–717.
21. Grafstein, B., and I. C. McQuarrie. 1978. Role of the nerve cell body in axonal regeneration. *In* Neuronal Plasticity. C. W. Cotman, editor. Raven Press, New York. 155–195.
22. Griffin, J. W., D. B. Drachman, and D. L. Price. 1976. Fast axonal transport in motor nerve regeneration. *J. Neurobiol.* 7:355–370.
23. Hasty, D. L., and E. D. Hay. 1978. Freeze-fracture studies of the developing cell surface. II. Particle-free membrane membrane blisters on glutaraldehyde-fixed corneal fibroblasts are artifacts. *J. Cell Biol.* 78:756–768.
24. Kreutzberg, G. W., and P. Schubert. 1971. Changes in axonal flow during regeneration of mammalian motor nerves. *Acta Neuropathol. Suppl.* V:70–75.
25. Lentz, T. L. 1972. Distribution of leucine-$^3$H during axoplasmic transport within regenerating neurons as determined by electron-microscope radioautography. *J. Cell Biol.* 52: 719–732.
26. Miani, N. 1960. Proximo-distal movement along the axon of protein synthesized in the perikaryon of regenerating neurons. *Nature (Lond.)* 185:541.
27. Murray, M. 1976. Regeneration of retinal axons into the goldfish optic tectum. *J. Comp. Neurol.* 168:175–196.
28. Pfenninger, K. H., and R. P. Bunge. 1974. Freeze-fracturing of nerve growth cones and young fibers: a study of developing plasma membrane. *J. Cell Biol.* 63:180–196.
29. Pfenninger, K. H., and M.-F. Maylié-Pfenninger. 1975. Distribution and fate of lectin binding sites on the surface of growing neuronal processes. *J. Cell Biol.* 67(2, Pt. 2):332 *a* (Abstr.).
30. Salpeter, M. M. 1966. General area of autoradiography at the electron microscope level. *Methods Cell Physiol.* 2:229–253.
31. Salpeter, M. M., L. Bachman, and E. E. Salpeter. 1969. Resolution in electron microscope radioautography. *J. Cell Biol.* 41:1–20.
32. Salpeter, M. M., and M. Szabo. 1972. Sensitivity in electron microscope autoradiography. I. The effect of radiation dose. *J. Histochem. Cytochem.* 20:425–434.
33. Schwartz, J. H. 1979. Axonal transport: components, mechanisms and specificity. *Annu. Rev. Neurosci.* 2:467–504.
34. Sturgess, J., M. Moscarello, and H. Schacter. 1978. The structure and biosynthesis of membrane glycoproteins. *Current Top. Membr. Transp.* 11:15–105.
35. Tessler, A. R., L. Autilio-Gambetti, and P. Gambetti. 1977. The distribution of axonally transported glycoproteins in regenerating axons. *J. Neuropathol. Exp. Neurol.* 36:634 (Abstr.).
36. Thompson, E. B., J. M. Schwartz, and E. R. Kandel. 1976. A radioautographic analysis in the light and electron microscope of identified *Aplysia* neurons and their processes after intrasomatic injection of L-[$^3$H]fucose. *Brain Res.* 112:251–281.